

CONFIDENTIAL NASA TM X-604



Declassified by authority of NASA  
Classification Change Notices No. *00043*  
Dated \*\**2-14-88*

# TECHNICAL MEMORANDUM

X-604

WIND-TUNNEL INVESTIGATION

OF THE STATIC LONGITUDINAL AERODYNAMIC CHARACTERISTICS OF  
MODELS OF REENTRY AND ATMOSPHERIC-ABORT CONFIGURATIONS OF  
A PROPOSED APOLLO SPACECRAFT AT MACH NUMBERS

FROM 0.30 TO 1.20

By Albin O. Pearson

Langley Research Center  
Langley Air Force Base, Virginia

NATIONAL AERONAUTICS AND SPACE ADMINISTRATION  
WASHINGTON

September 1961

CONFIDENTIAL

NASA TM X-604

CONFIDENTIAL

NATIONAL AERONAUTICS AND SPACE ADMINISTRATION

TECHNICAL MEMORANDUM X-604

WIND-TUNNEL INVESTIGATION

OF THE STATIC LONGITUDINAL AERODYNAMIC CHARACTERISTICS OF  
MODELS OF REENTRY AND ATMOSPHERIC-ABORT CONFIGURATIONS OF  
A PROPOSED APOLLO SPACECRAFT AT MACH NUMBERS

FROM 0.30 TO 1.20\*

By Albin O. Pearson

SUMMARY

An investigation has been conducted in the Langley 8-foot transonic pressure tunnel to determine the static longitudinal aerodynamic characteristics of models of reentry and atmospheric-abort configurations of a proposed Apollo spacecraft. Two atmospheric-abort configurations with tower support rods of different length were tested. The tests were conducted at angles of attack from about  $-2^{\circ}$  to  $182^{\circ}$  for the reentry configuration and from approximately  $-2^{\circ}$  to  $50^{\circ}$  for the atmospheric-abort configurations. The test Reynolds number, based on maximum body diameter and free-stream conditions, varied from about  $1.64 \times 10^6$  to  $3.83 \times 10^6$ .


The results of this investigation have shown that the reentry configuration is stable at angles of attack to about  $50^{\circ}$  and also at angles of attack greater than approximately  $130^{\circ}$ . Depending upon Mach number, this configuration trims in the stable regions at angles of attack from about  $20^{\circ}$  to  $32^{\circ}$  and from  $145^{\circ}$  to  $155^{\circ}$ . The atmospheric-abort configuration, with either the long or the short tower, was statically stable at angles of attack near  $0^{\circ}$  at Mach numbers greater than about 0.60.

INTRODUCTION

A wind-tunnel research program has been initiated by the National Aeronautics and Space Administration to investigate the static longitudinal aerodynamic characteristics of models of reentry and

---

\*Title, Unclassified.



CONFIDENTIAL

atmospheric-abort configurations of a proposed Apollo spacecraft. The results of one of these investigations at supersonic speeds are given in reference 1.

The present investigation was performed in the Langley 8-foot transonic pressure tunnel and provides information at subsonic and transonic speeds on 0.07-scale models of reentry and atmospheric-abort configurations. Two atmospheric-abort configurations with tower support rods of different length were tested. The tests were conducted at angles of attack from about  $-2^\circ$  to  $182^\circ$  for the reentry configuration and from approximately  $-2^\circ$  to  $50^\circ$  for the atmospheric-abort configurations. The test Reynolds number, based on maximum body diameter and free-stream conditions, varied from about  $1.64 \times 10^6$  to  $3.83 \times 10^6$ .

### SYMBOLS

The data presented herein are referred to the body system of axes with the origin located at the center of gravity of the various configurations tested. The positive direction of forces, moments, and displacements are shown in figure 1. The coefficients and symbols are defined as follows:

A	maximum cross-sectional area, 0.6504 sq ft
$C_A$	axial-force coefficient, $\frac{\text{Axial force}}{qA}$
$C_A, C_{m \approx 0}$	axial-force coefficient at $C_m \approx 0$ ( $0^\circ < \alpha < 50^\circ$ )
$C_m$	pitching-moment coefficient, $\frac{\text{Pitching moment}}{qAd}$
$C_{m\alpha}$	slope of pitching-moment curve at $C_m \approx 0$ ( $0^\circ < \alpha < 50^\circ$ ), $\partial C_m / \partial \alpha$ , per deg
$C_N$	normal-force coefficient, $\frac{\text{Normal force}}{qA}$
$C_{N\alpha}$	slope of normal-force curve at $C_m \approx 0$ ( $0^\circ < \alpha < 50^\circ$ ), $\partial C_N / \partial \alpha$ , per deg
$C_{p,c}$	model chamber-pressure coefficient, $\frac{\text{Model chamber pressure} - \text{Free-stream static pressure}}{q}$

L  
1  
8  
1  
6

DECLASSIFIED

3

D diameter, in.  
d maximum body diameter, 10.920 in.  
M free-stream Mach number  
q free-stream dynamic pressure, lb/sq ft  
r radius, in.  
 $\alpha$  angle of attack of model center line, deg


### MODELS, TESTS, AND ACCURACY

Details of the 0.07-scale models and components tested are shown in figure 2 and photographs are presented in figure 3. Two models, both of which were conical bodies of revolution, were used in the tests of the reentry configuration. A model made of wood was used for angles of attack up to about  $90^\circ$  whereas an aluminum-alloy model was used at angles of attack greater than  $90^\circ$ . The two abort systems tested were attached to the conical end of the aluminum-alloy reentry configuration and were composed of a cylindrical aluminum-alloy body, simulating a rocket container, mounted on a tower made from three cross-braced steel rods. The three rods were located  $120^\circ$  apart and were oriented so that the two lower rods were in a horizontal plane when the model was near an angle of attack of  $0^\circ$ .

The models were mounted on a three-component internally located strain-gage balance which was sting-supported. Several model-sting-support arrangements were used in order to obtain a large angle-of-attack range and also to maintain the models near the tunnel center line throughout this range. (See fig. 3.)

The tests were conducted in the Langley 8-foot transonic pressure tunnel at a stagnation pressure near 1.0 atmosphere and at such a dew-point temperature that the airflow was free of condensation shocks. The variation of Reynolds number, based on model maximum diameter and free-stream conditions, with Mach number is shown in figure 4. The models were tested at Mach numbers from 0.30 to 1.20 at angles of attack from about  $-2^\circ$  to  $182^\circ$  for the reentry configuration and from approximately  $-2^\circ$  to  $50^\circ$  for the abort configurations.

Normal force, axial force, and pitching moment were determined by means of the strain-gage balance with the pitching moments referred to the center-of-gravity locations shown in figure 2. The axial-force results presented herein are gross values and have not been adjusted to



CONFIDENTIAL

a condition of free-stream static pressure at the model base. The model chamber pressure was measured by means of an orifice located inside the model in the strain-gage balance chamber.

Based upon balance accuracy (neglecting any sting-interference effects), it is estimated that the coefficients of normal force, axial force, and pitching moment are accurate within  $\pm 0.046$ ,  $\pm 0.046$ , and  $\pm 0.0085$ , respectively, at a Mach number of 0.30 and are accurate within  $\pm 0.007$ ,  $\pm 0.007$ , and  $\pm 0.0012$ , respectively, at a Mach number of 1.20. All data presented from this investigation are essentially free of wall-reflected disturbances. The maximum variation of the actual test Mach numbers from the presented nominal values is less than  $\pm 0.005$ . Corrections were applied for tunnel flow angularity and for structural deflections of the model sting and balance. The accuracy of the angle of attack is estimated to be within  $\pm 0.20^\circ$ .


#### PRESENTATION OF RESULTS AND DISCUSSION

It is shown in reference 2, for models and sting-support systems similar to those of the present investigation, that some interference effects due to sting-support arrangements are indicated at the higher angles of attack. These effects, for the model of reference 1, are negligible on the pitching-moment and axial-force characteristics, and for the normal-force coefficients are a maximum of about 4 percent of the presented faired values. Although the models of the present investigation are not identical to those of reference 1, the interference effects are expected to be essentially the same in magnitude.

The pitching-moment, normal-force, axial-force, and chamber-pressure coefficients of the various configurations investigated are presented in figures 5 and 6 and summaries of the aerodynamic characteristics are shown in figure 7.

The reentry configuration is statically stable at angles of attack to about  $50^\circ$  and also at angles of attack greater than approximately  $130^\circ$  (fig. 5(a)). Depending upon Mach number, this configuration trims in the stable regions at angles of attack from about  $20^\circ$  to  $32^\circ$  and from  $145^\circ$  to  $155^\circ$ . A trim condition also exists in the unstable region at angles of attack greater than about  $77^\circ$ .

The atmospheric-abort configuration with either the long or the short tower (fig. 7(b)) is statically stable near an angle of attack of  $0^\circ$  at Mach numbers greater than about 0.60 but is statically unstable for all Mach numbers at the higher angles of attack (fig. 6(a)). The axial-force coefficients at all angles of attack were essentially the



DECLASSIFIED

CONFIDENTIAL

5

same for both the long and short tower models, but the slope of the normal-force curve was less for the short tower model.

#### CONCLUDING REMARKS

The results of wind-tunnel tests of reentry and atmospheric-abort configurations of a proposed Apollo spacecraft, conducted in the Langley 8-foot transonic pressure tunnel at Mach numbers from 0.30 to 1.20, have shown that the reentry configuration is statically stable at angles of attack to about  $50^\circ$  and also at angles of attack greater than approximately  $130^\circ$ . Depending upon Mach number, this configuration trims in the stable regions at angles of attack from about  $20^\circ$  to  $32^\circ$  and from  $145^\circ$  to  $155^\circ$ . The atmospheric-abort configuration, with either the long or short tower, is statically stable at angles of attack near  $0^\circ$  at Mach numbers greater than about 0.60.

Langley Research Center,  
National Aeronautics and Space Administration,  
Langley Air Force Base, Va., August 4, 1961.

#### REFERENCES

1. Morgan, James R., and Fournier, Roger H.: Static Longitudinal Aerodynamic Characteristics of a 0.07-Scale Model of a Proposed Apollo Spacecraft at Mach Numbers of 1.57 to 4.65. NASA TM X-603, 1961.
2. Pearson, Albin O.: Wind-Tunnel Investigation at Mach Numbers From 0.50 to 1.14 of the Static Aerodynamic Characteristics of a Model of a Project Mercury Capsule. NASA TM X-292, 1960.



03171230030

CONFIDENTIAL

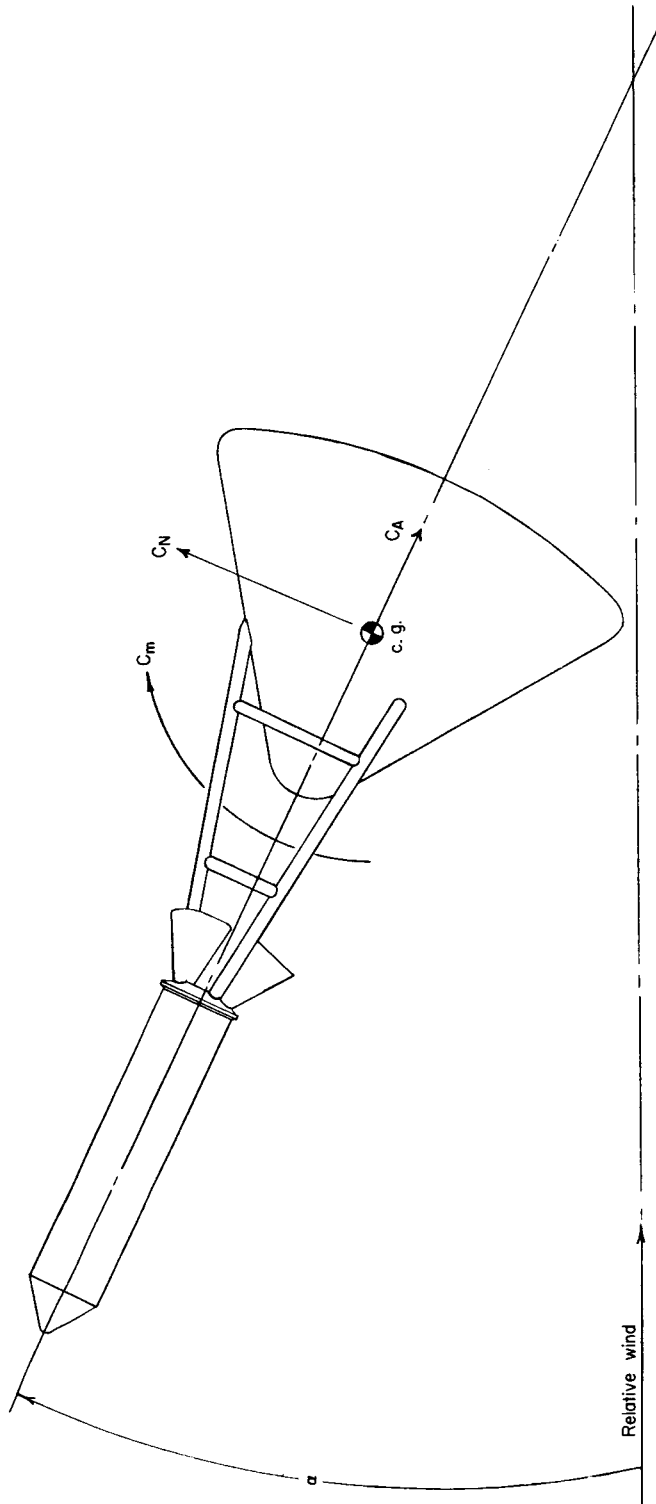
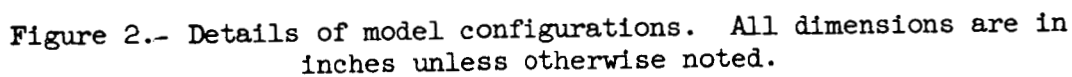


Figure 1.- Body system of axes. Arrows indicate positive direction. (Atmospheric-abort configuration with short tower shown.)

CONFIDENTIAL

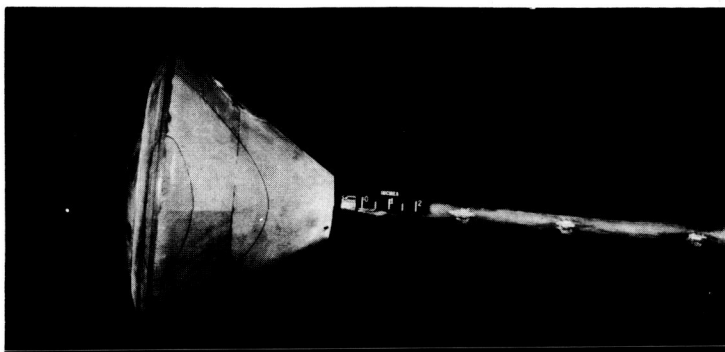
IL-1816



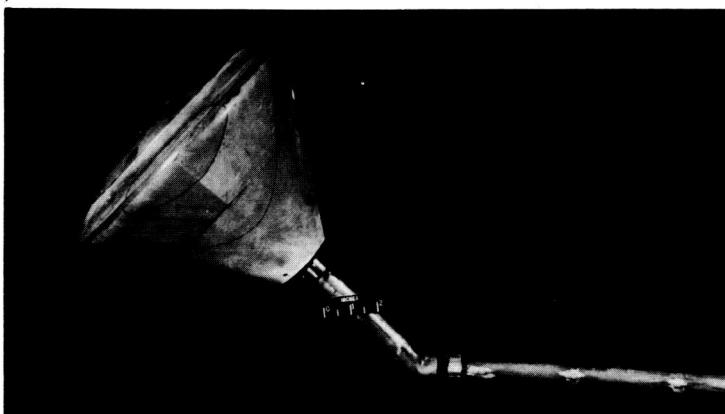


0317132A1030

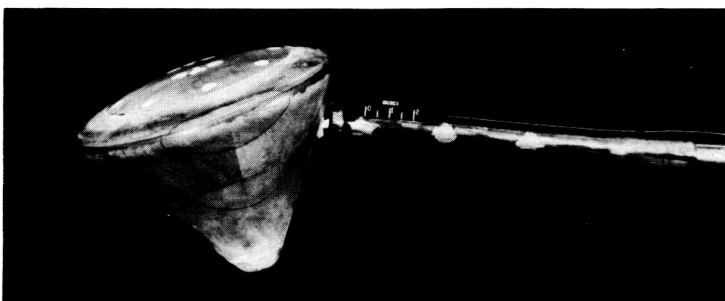
CONFIDENTIAL

 $\alpha \approx -2^\circ \text{ to } 20^\circ$ 

L-61-4882

 $\alpha \approx 30^\circ \text{ to } 50^\circ$ 

L-61-4881

 $\alpha \approx 60^\circ \text{ to } 80^\circ$ 

(a) Reentry configuration.

L-61-4883

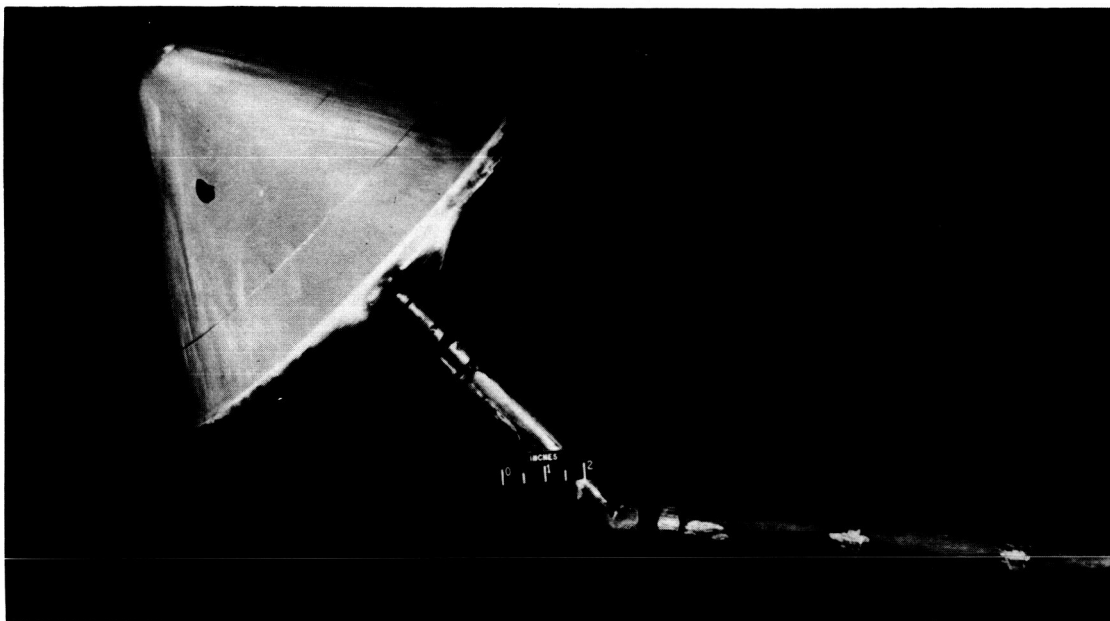
Figure 3.- Model configurations and sting-support arrangements.

L-1816

DECLASSIFIED

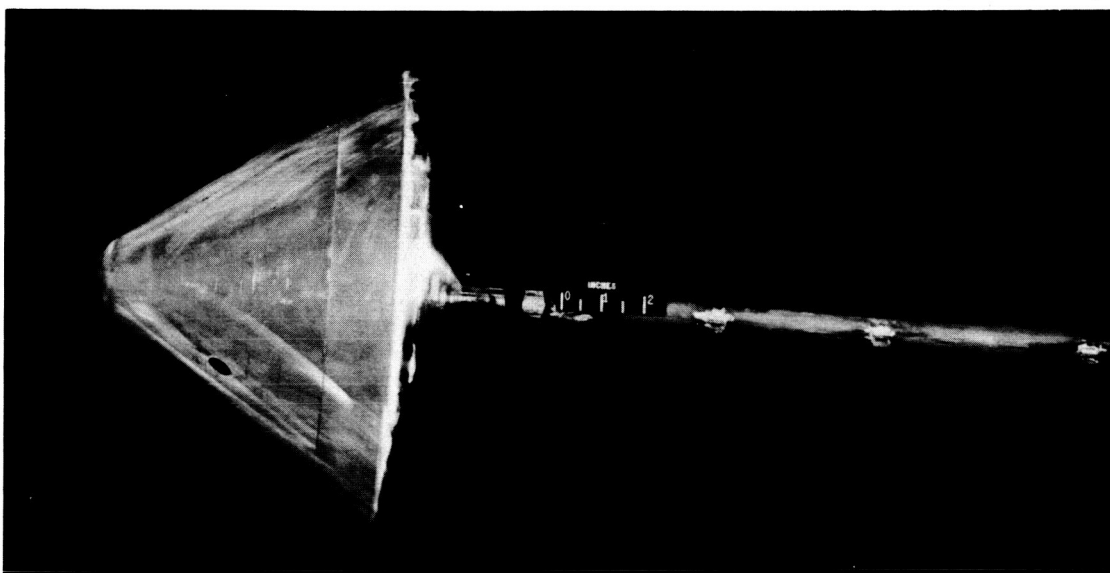
CONFIDENTIAL

9



$\alpha \approx 130^\circ$  to  $150^\circ$

L-61-4885



$\alpha \approx 160^\circ$  to  $182^\circ$

(a) Reentry configuration. Concluded.

L-61-4884

Figure 3.- Continued.

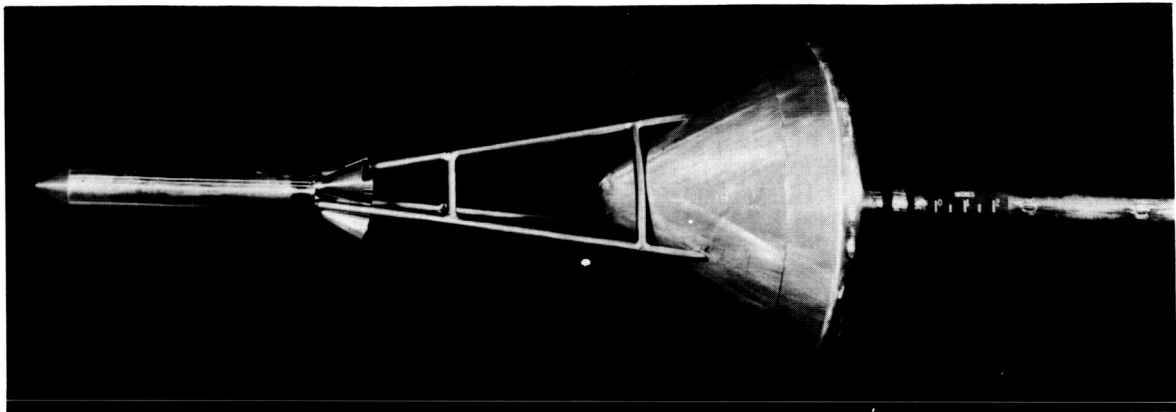


L-1816

031710201030

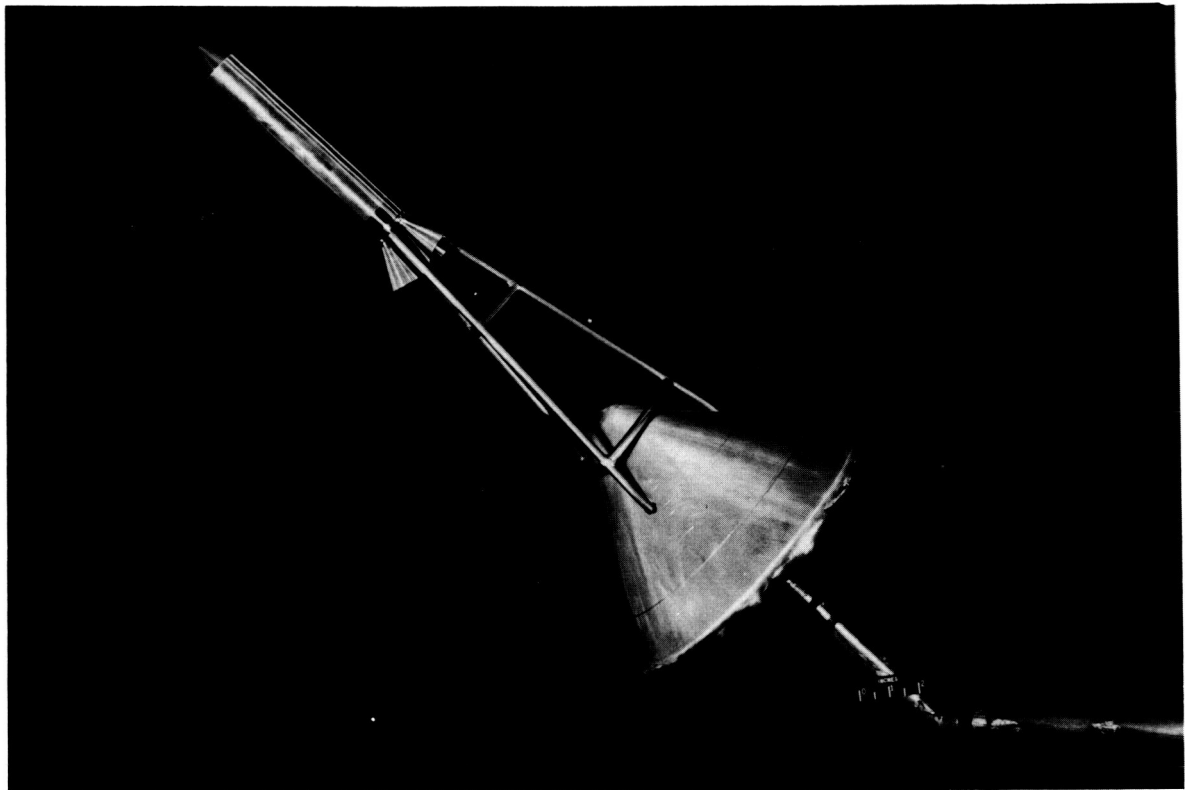
10

CONFIDENTIAL



$\alpha \approx -2^\circ \text{ to } 20^\circ$

L-61-4886



$\alpha \approx 30^\circ \text{ to } 50^\circ$

L-61-4888

(b) Atmospheric-abort configuration. (Long tower shown.)

Figure 3.- Concluded.

L-1816

DECLASSIFIED

CONFIDENTIAL

11

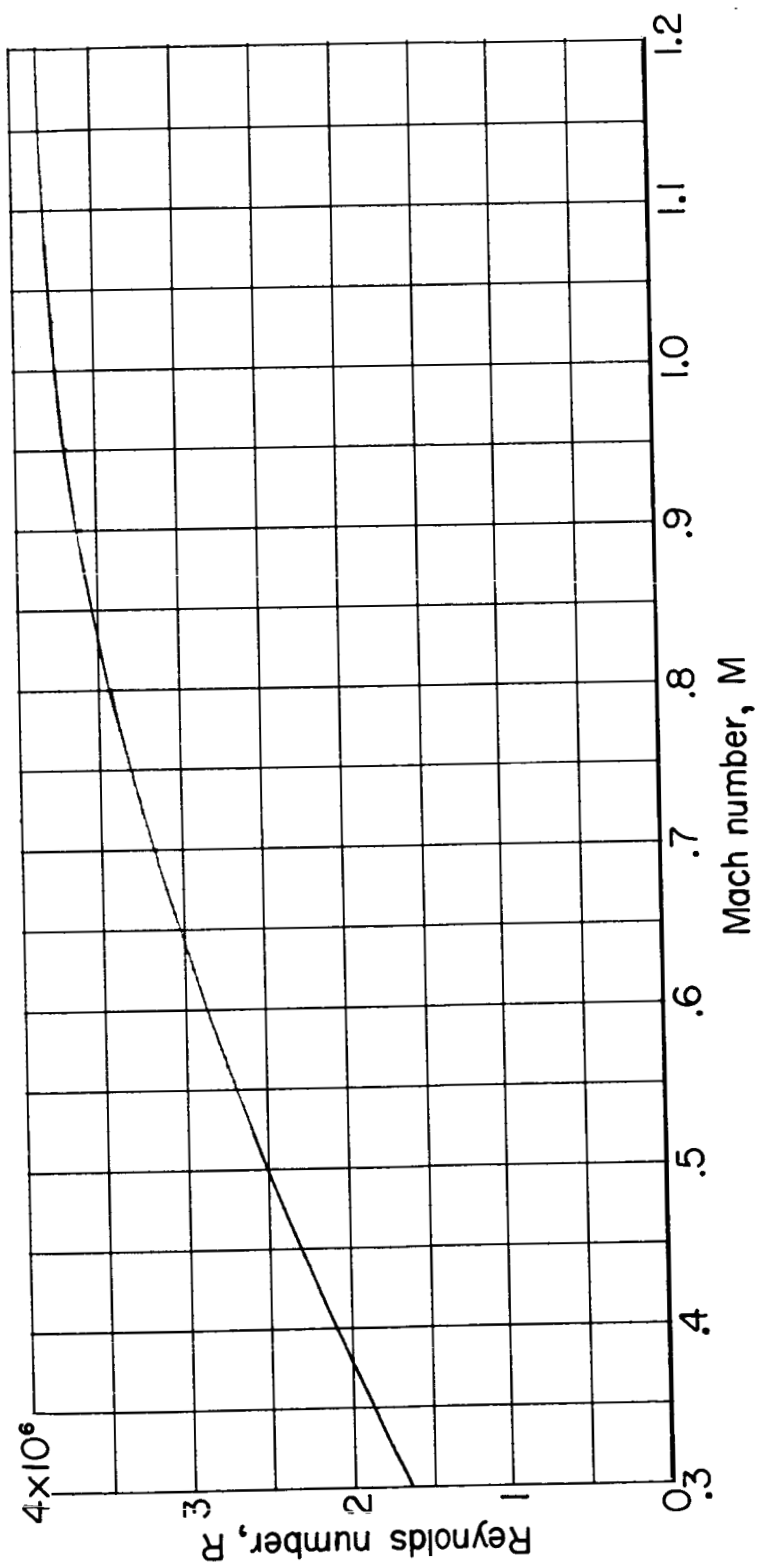
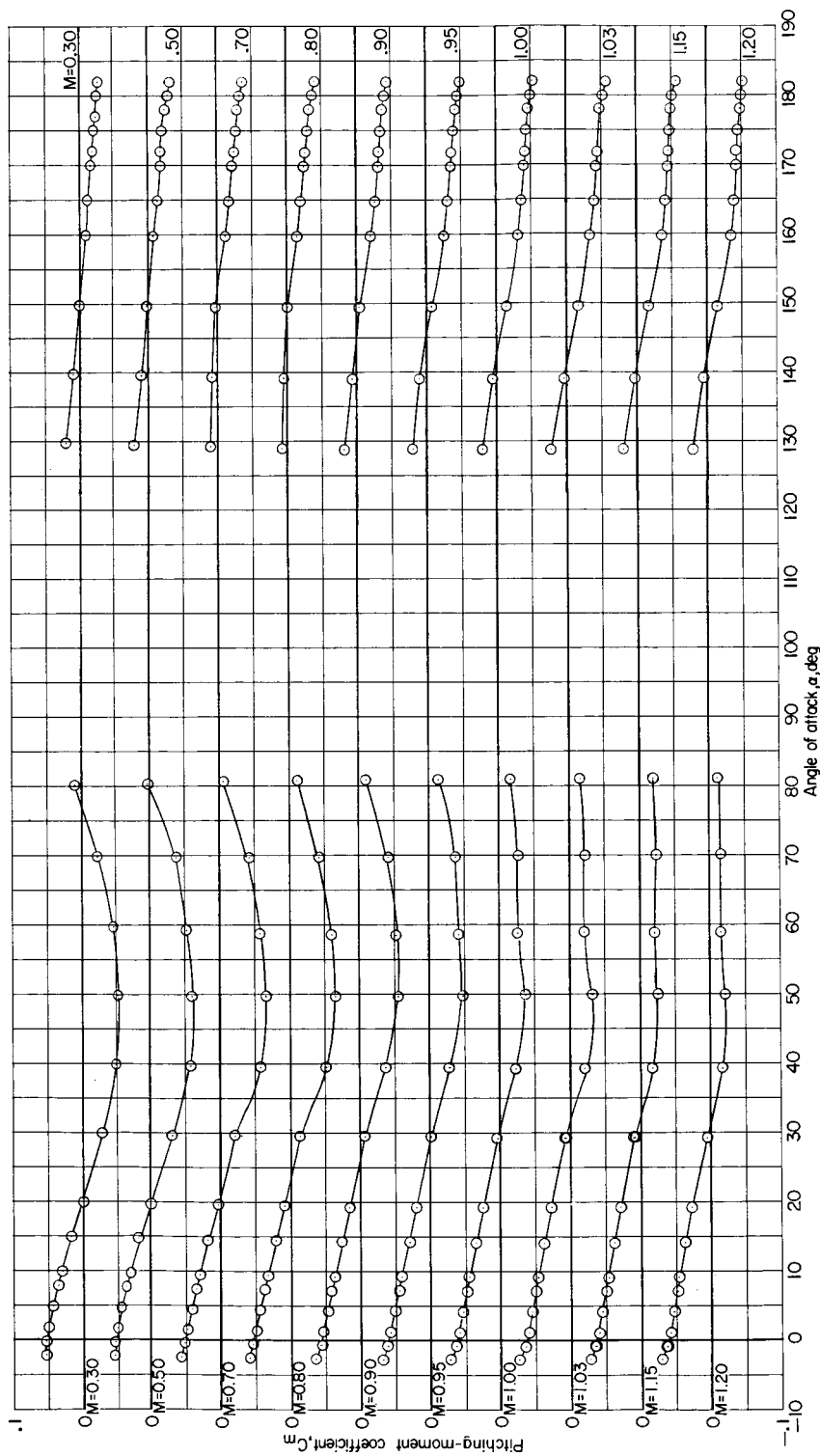


Figure 4.- Variation of Reynolds number, based on model diameter of 10.920 inches and free-stream conditions, with Mach number.

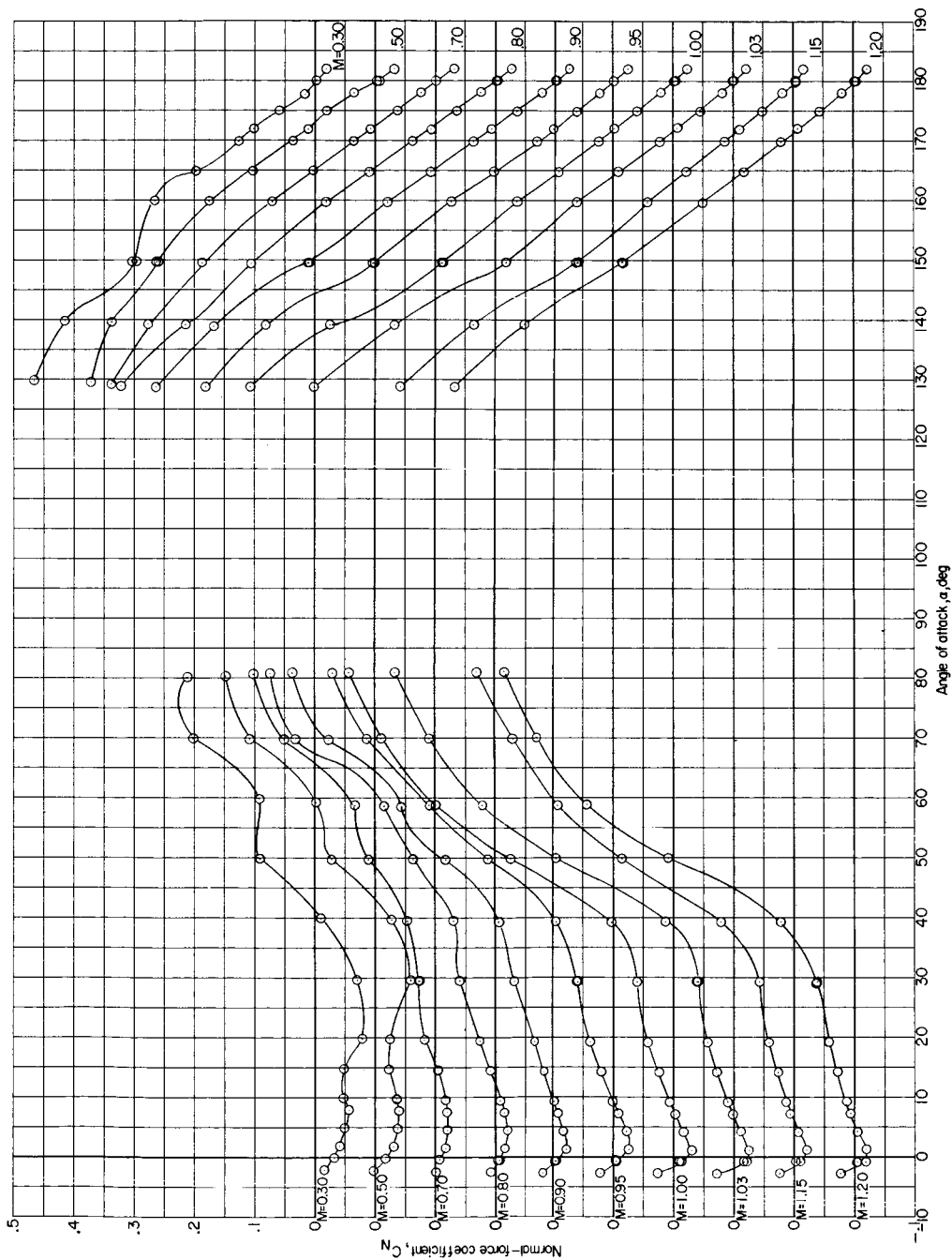
CONFIDENTIAL



(a) Variation of  $C_m$  with  $\alpha$ .

Figure 5.- Variation of static longitudinal aerodynamic characteristics of model. Reentry configuration.

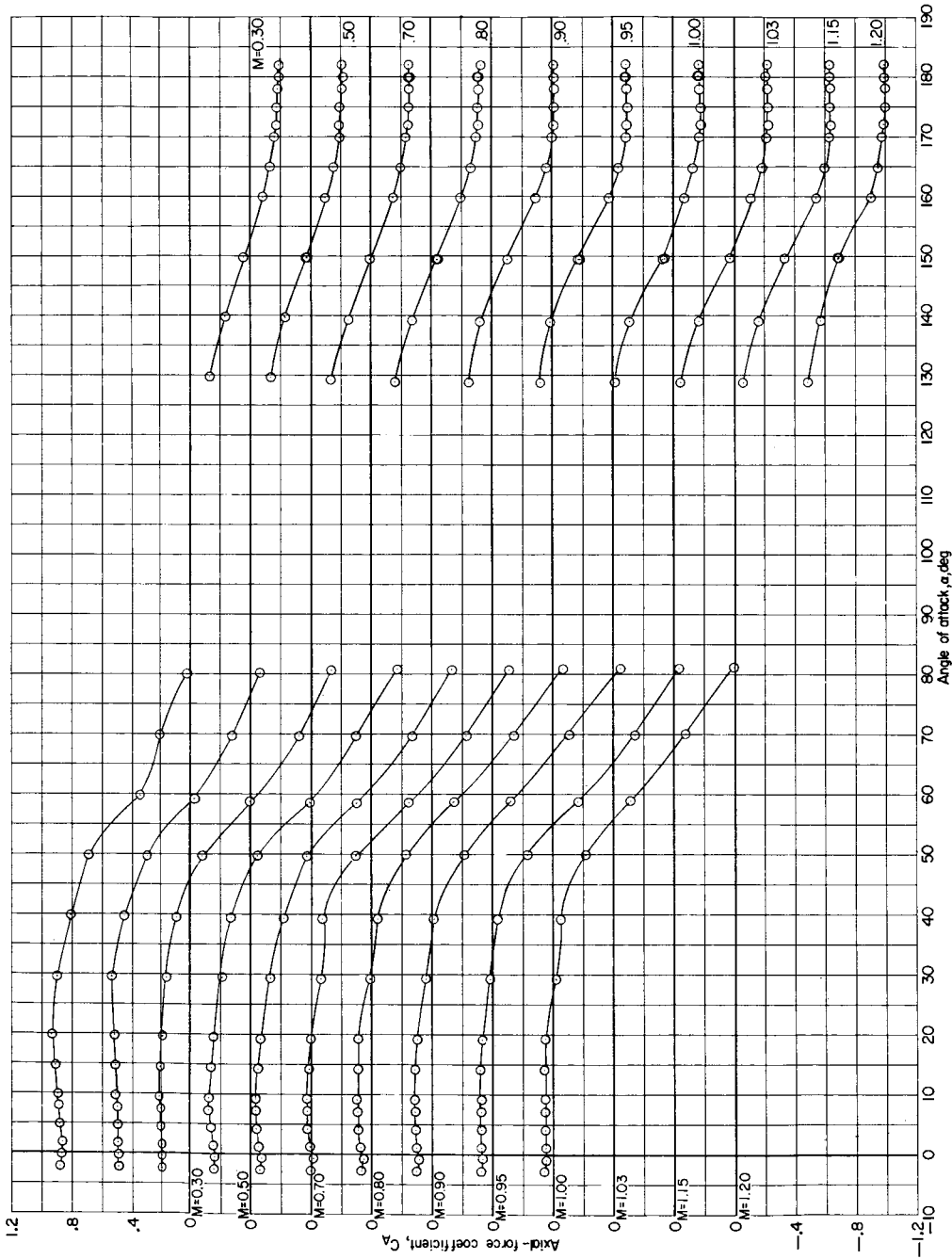
L-1816



(b) Variation of  $C_N$  with  $\alpha$ .

Figure 5.- Continued.

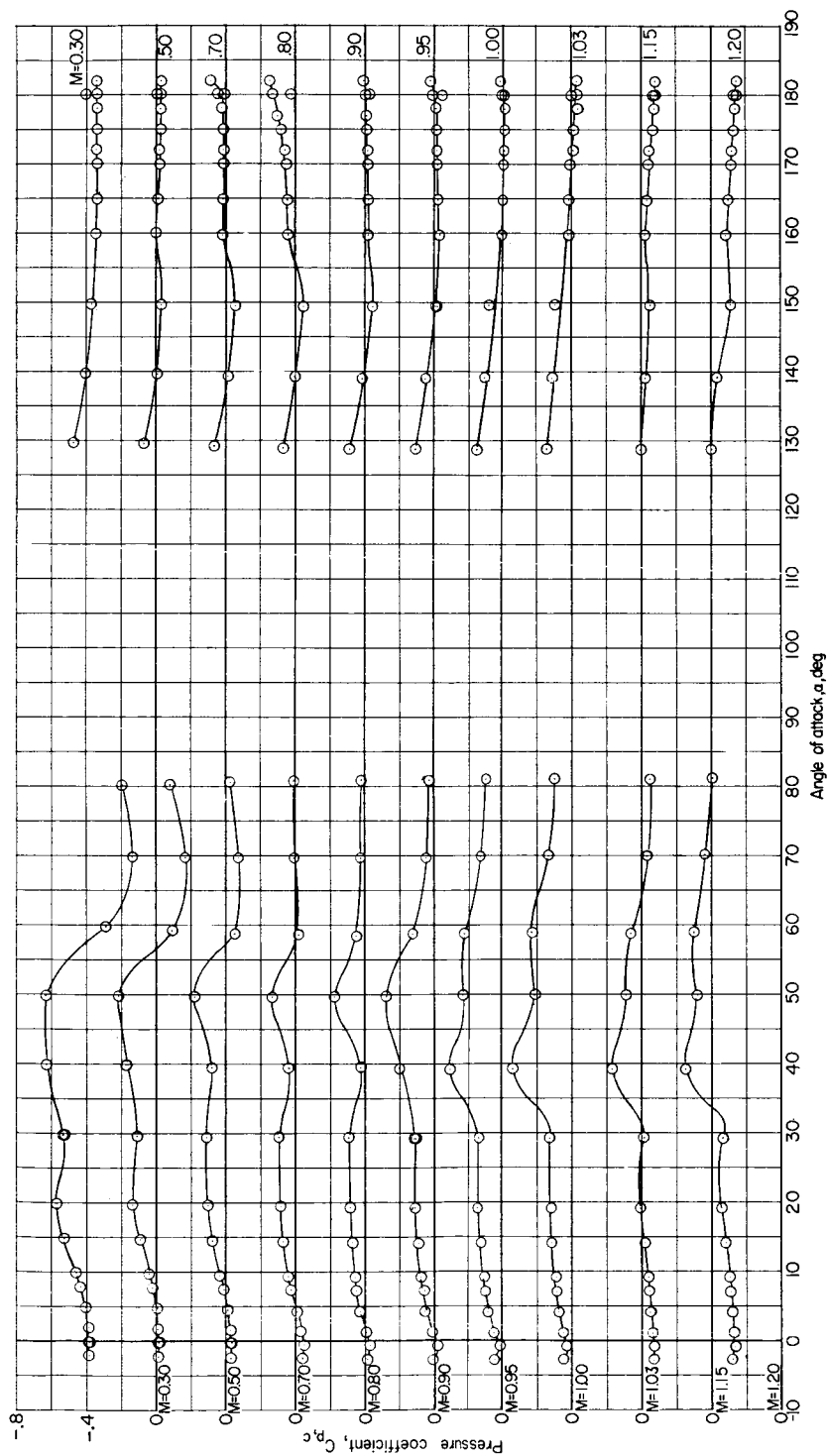
CONFIDENTIAL



(c) Variation of  $C_A$  with  $\alpha$ .

Figure 5.- Continued.

CONFIDENTIAL

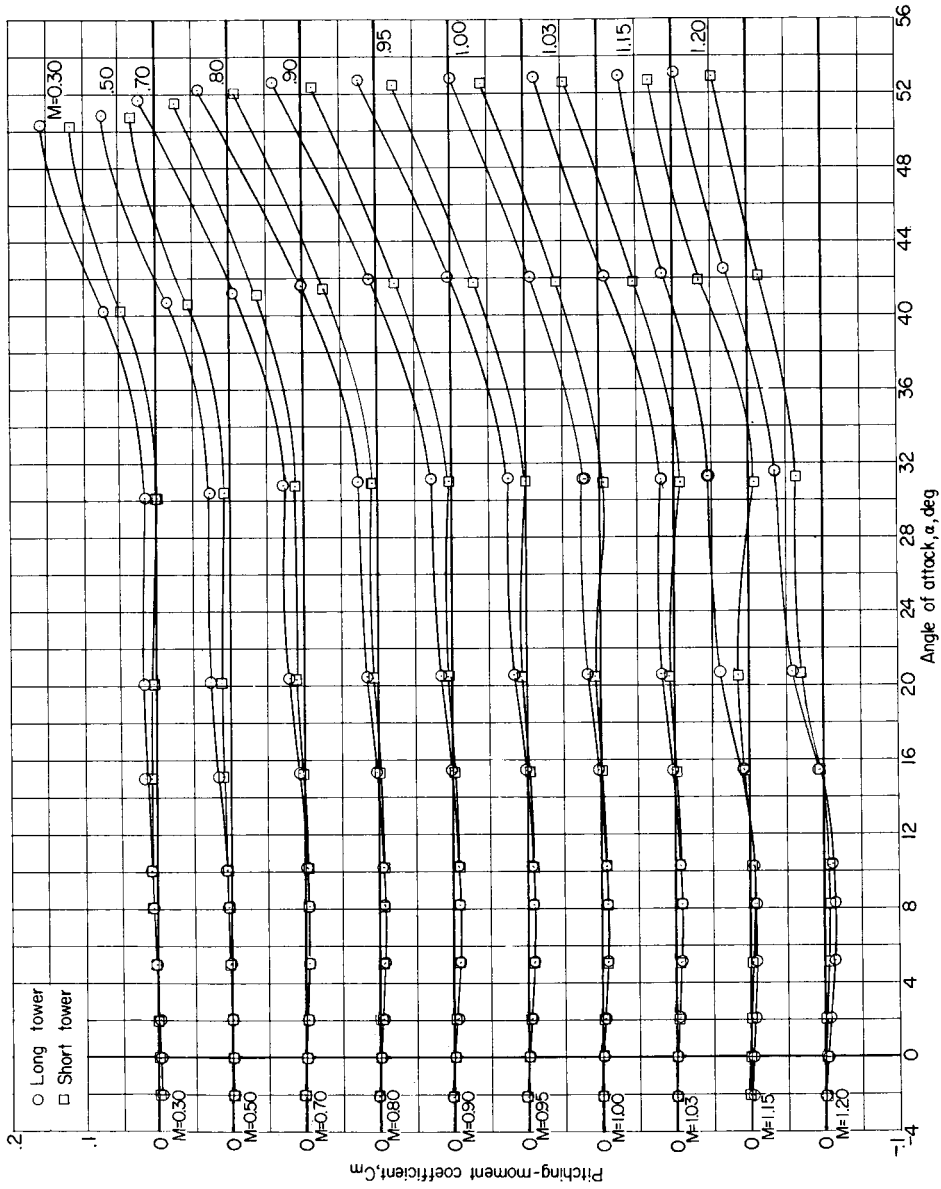


(d) Variation of  $C_{p,c}$  with  $\alpha$ .

Figure 5.- Concluded.



CONFIDENTIAL

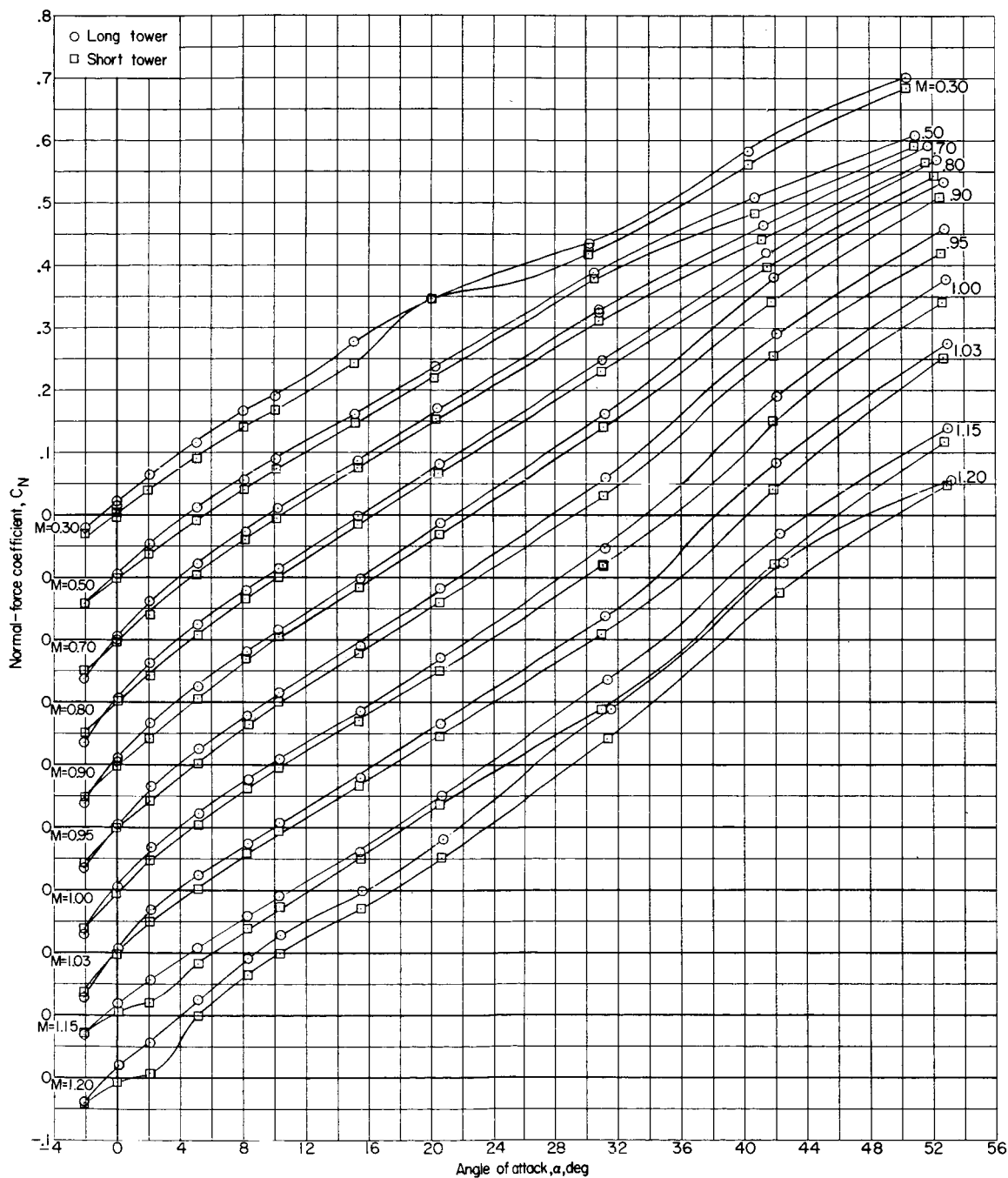


(a) Variation of  $C_m$  with  $\alpha$ .

Figure 6.- Variation of static longitudinal characteristics of model. Atmospheric-abort configurations.

CONFIDENTIAL

17



(b) Variation of  $C_N$  with  $\alpha$ .

Figure 6.- Continued.

CONFIDENTIAL

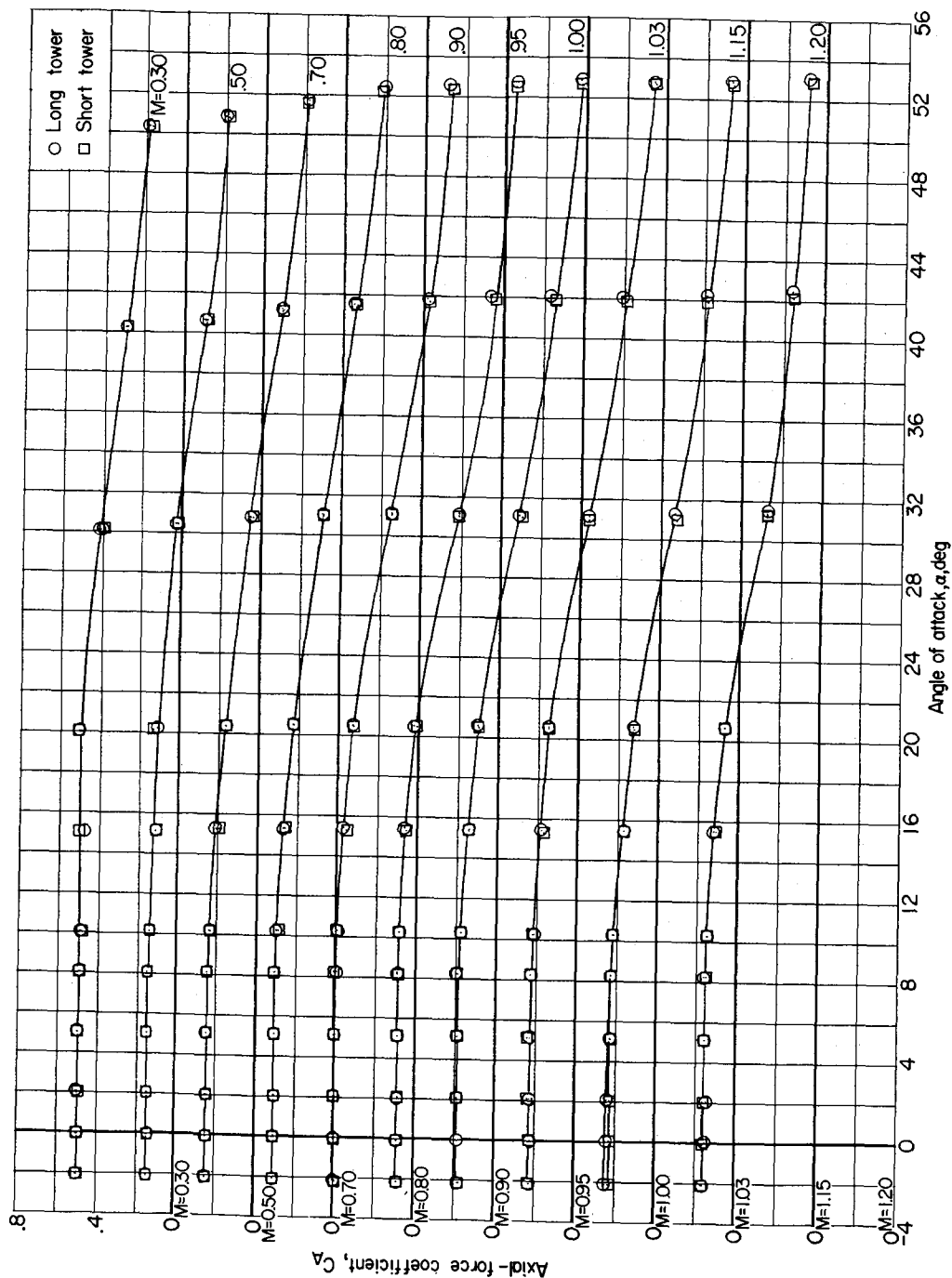
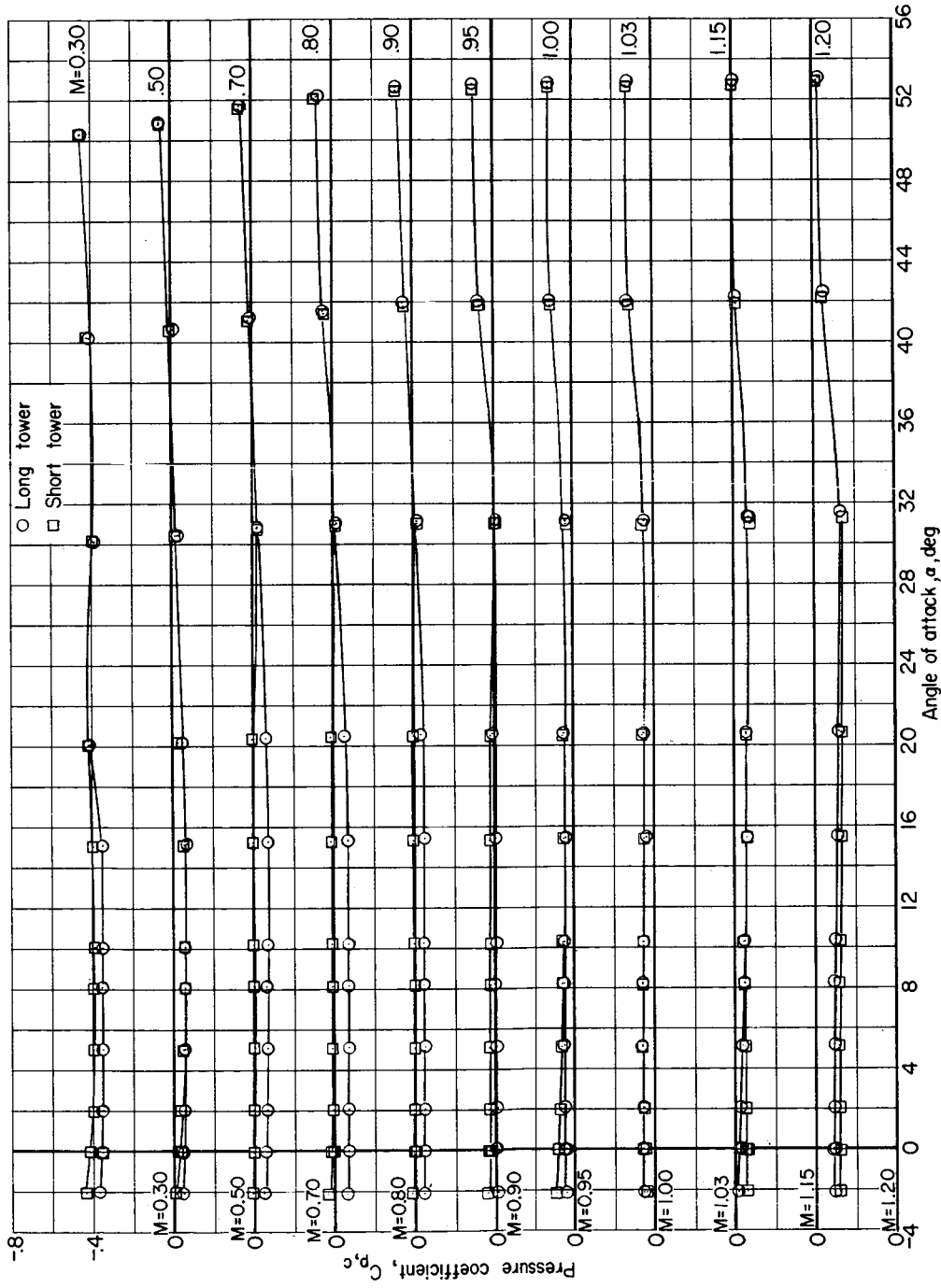
(c) Variation of  $C_A$  with  $\alpha$ .

Figure 6.- Continued.

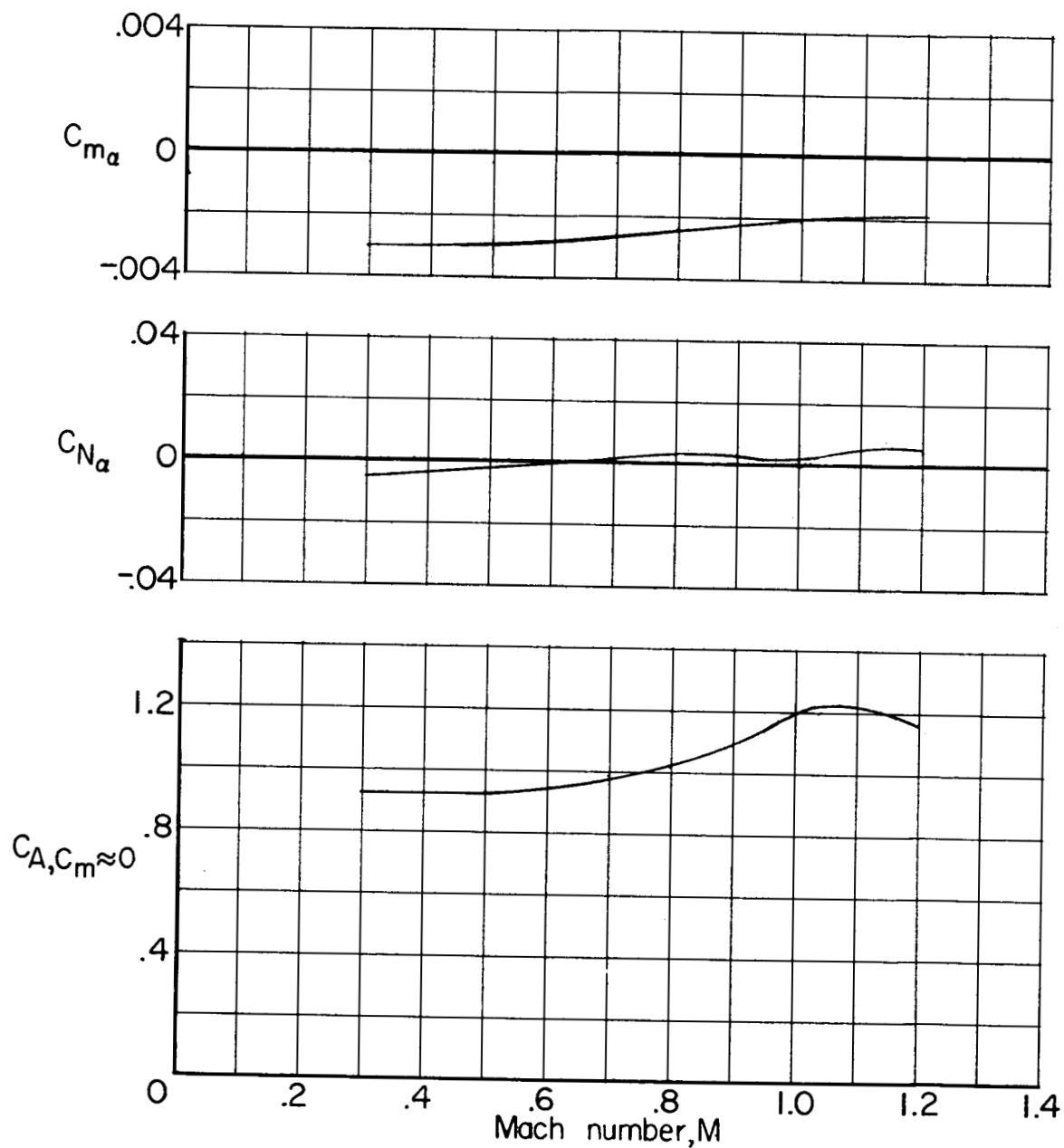
CONFIDENTIAL



(d) Variation of  $C_{p,c}$  with  $\alpha$ .

Figure 6.- Concluded.

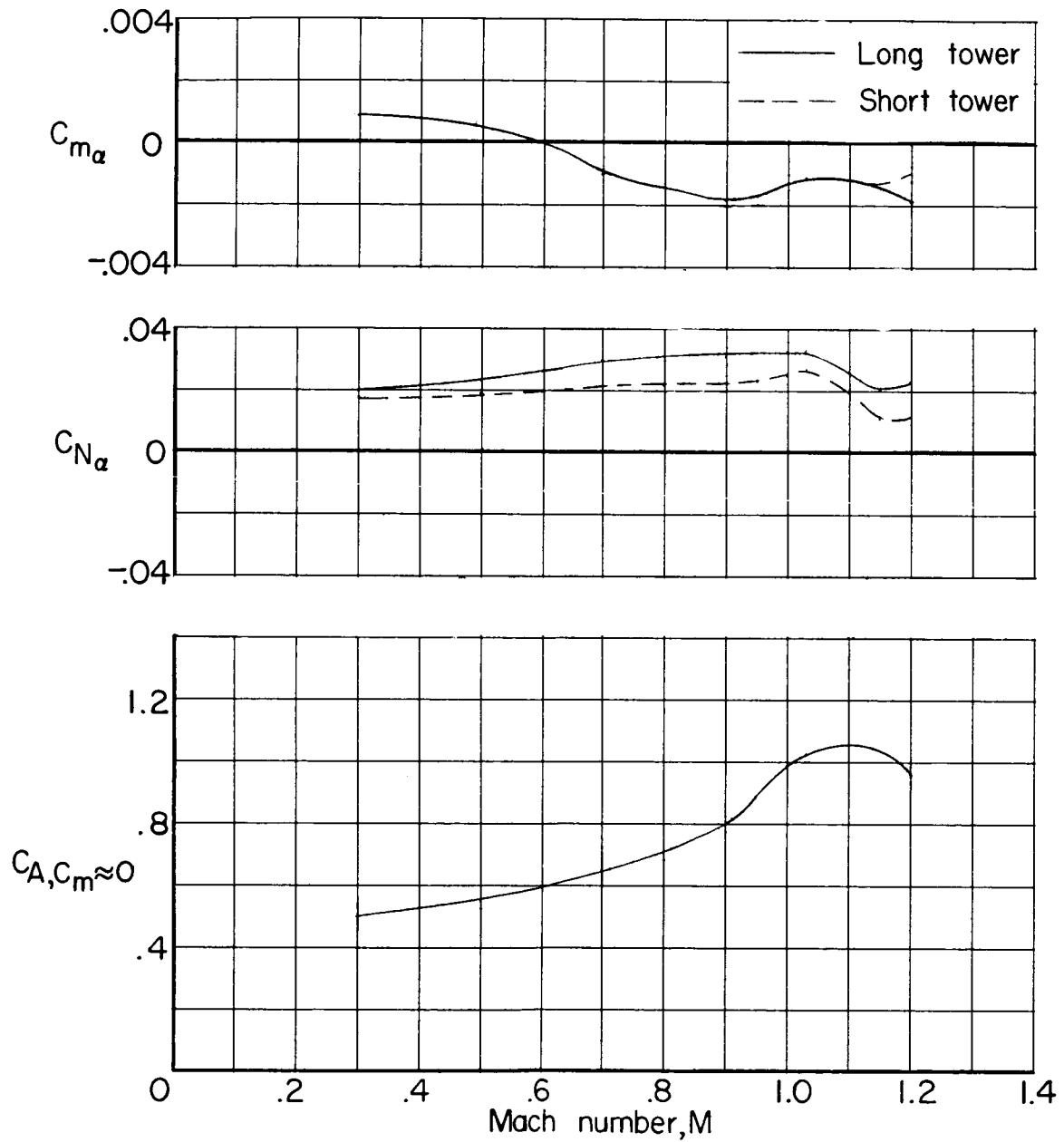
CONFIDENTIAL



(a) Reentry configuration.

Figure 7.- Summary of static longitudinal aerodynamic characteristics of models.

DECLASSIFIED



(b) Atmospheric-abort configurations.

Figure 7.- Concluded.